HIPPOCAMPUS 15:867–873 (2005)

Phase Precession of Medial Prefrontal Cortical Activity Relative to the Hippocampal Theta Rhythm

Matthew W. Jones and Matthew A. Wilson*

ABSTRACT: Theta phase-locking and phase precession are two related phenomena reflecting coordination of hippocampal place cell firing with the local, ongoing theta rhythm. The mechanisms and functions of both the phenomena remain unclear, though the robust correlation between firing phase and location of the animal has lead to the suggestion that this phase relationship constitutes a temporal code for spatial information. Recent work has described theta phase-locking in the rat medial prefrontal cortex (mPFC), a structure with direct anatomical and functional links to the hippocampus. Here, we describe an initial characterization of phase precession in the mPFC relative to the CA1 theta rhythm. mPFC phase precession was most robust during behavioral epochs known to be associated with enhanced theta-frequency coordination of CA1 and mPFC activities. Precession was coherent across the mPFC population, with multiple neurons precessing in parallel as a function of location of the animal. The existence of phase precession beyond the hippocampus implies a more global role for this phenomenon during theta rhythm-mediated coordination of neural activity. © 2005 Wiley-Liss, Inc.

KEY WORDS: spatial learning; local field potential; synchrony

INTRODUCTION

Rodent spatial behaviors are consistently associated with two electrophysiological signatures in the hippocampus. The first is the prominence of the theta rhythm, a 4–12 Hz oscillation in the hippocampal local field potential generated by the synchronized activities of inhibitory and excitatory populations (Vanderwolf, 1969; Buzsaki, 2002). Beyond spatial exploration in rodents, theta rhythms arise during other complex behaviors presumed to require mnemonic processing or decision-making, such as working memory in primates (Lee et al., 2005) and navigation and working memory in humans (Kahana et al., 1999; Raghavachari et al., 2001). A second hippocampal hallmark is that the firing rate of place cells—hippocampal principal excitatory neurons with spatial receptive fields ("place fields")—conveys spatial information (O'Keefe and Dostrovsky, 1971). The firing rates of place cell ensembles can therefore be used to predict the location of an animal (Wilson and McNaughton, 1993).

The theta rhythm and underlying hippocampal firing rates are coupled by the characteristic temporal relationship between place cell spike-timing and the phase of the concurrent theta cycle: place cell spikes are "phase-locked" to theta (Buzsaki and Eidelberg, 1983). Thus, the spikes of a given neuron are not distributed randomly across the theta cycle. Rather, they consistently tend to occur during a restricted phase of the oscillation. Furthermore, in CA1, CA3, and the dentate gyrus, phase-locking to the local theta rhythm is accompanied by the related phenomenon of phase precession: each neuron tends to fire on progressively earlier phases of the concurrent theta cycle as an animal moves through its place field (O'Keefe and Recce, 1993). Intuitively, phase precession must therefore blur phase-locking, but the extent to which the two phenomena are mechanistically distinct or can be decoupled has not yet been addressed experimentally.

Potential mechanisms and functions of phase-locking and phase-precession have been the subject of much debate. Some models suggest that the phenomena arise through the intrinsic biophysical properties of hippocampal neurons, and that precession is an inevitable consequence of a broader firing rate versus phase relationship (Lengyel et al., 2003). The majority of models incorporate oscillatory network dynamics, interplay between inhibition and excitation (Jensen and Lisman, 1996; Wallenstein and Hasselmo, 1997; Bose and Recce, 2001), and ramping-up of firing rate toward the peak of a place field (Harris et al., 2002; Mehta et al., 2002). A key issue is whether rate and phase can vary independently, leaving phase free to encode information beyond that carried by firing rate (Huxter et al., 2003). Either way, it is clear that the theta phase at which each spike occurs correlates well with the position of an animal within that cell's place field, and hence that phase can carry spatial information at a greater resolution than that imparted by firing rate alone.

Activity phase-locked to the hippocampal theta rhythm is not restricted to the hippocampal formation, and has been demonstrated in structures including cingulate cortex (Colom et al., 1988), amygdala (Pare and Gaudreau, 1996), entorhinal cortex (Frank et al., 2001), striatum (Berke et al., 2004), and visual cortex (Lee et al., 2005). However, phase precession in structures beyond the hippocampus has not yet been reported. Within the hippocampus itself, Skaggs et al. (1996) suggested that phase precession in CA3 and CA1 may be inherited to some extent from the dentate gyrus. They proposed that inheritance of pre-

Department of Brain and Cognitive Sciences, The Picower Institute for Learning and Memory, RIKEN-MIT Neuroscience Research Center, Massachusetts Institute of Technology, Cambridge, Massachusetts
Grant sponsor: The Wellcome Trust, UK; Grant sponsor: NIMH; Grant number: NIMH-R01 MH 61976.
*Correspondence to: Matthew Wilson, MIT Building E18-370, 77 Massachusetts Avenue, Cambridge, MA 02139. E-mail: mwilson@mit.edu
Accepted for publication 27 June 2005
DOI 10.1002/hipo.20119
Published online 7 September 2005 in Wiley InterScience (www.interscience.wiley.com).

cession from upstream regions requires adequate connectivity between the regions in question, plus synaptic time constants shorter than the ~100 ms theta cycle. These conditions may be satisfied in other structures that contain activity phase-locked to hippocampal theta rhythm and that are directly connected to the hippocampus. It therefore seems reasonable to expect some degree of theta phase precession in such regions.

Phase-locking to hippocampal theta has most recently been demonstrated in the medial prefrontal cortex (mPFC; Siapas et al., 2005). The hippocampal formation sends monosynaptic, glutamatergic projections to mPFC, and lesion studies implicate both CA1 and mPFC in spatial working memory. Our recent work (Jones and Wilson, 2005) demonstrates a behavioral dependence of mPFC theta phase-locking, showing that it may underlie coordinated interactions between CA1 and mPFC during spatial working memory and decision-making. We proposed that theta rhythms mediate the synchronization of CA1 and mPFC activities, allowing the integration of hippocampal spatial information into a broader, decision-making network. Here, we describe an initial characterization of phase precession in the rat mPFC during the same behavioral conditions—a spatial working memory task—that selectively enhance theta-frequency coordination between CA1 and mPFC.

METHODS

All procedures were performed in accordance with MIT Committee on Animal Care and NIH guidelines. Four male Long-Evans rats (2–6 months) were trained to run a continuous alternation task for food reward (Fig. 1A; maze dimensions 170 by 130 cm). Each trial comprised distinct sample and test epochs. During sample epochs, the rat ran toward the "forced-turn" end of the maze, and was directed down left or right arms by a moveable barrier. During test epochs, the rat ran back to the opposite, "choice" end of the maze and was required to choose between left or right arms according to the direction of his preceding turn at the forced-turn end. The contingency was set such that, for example, a rat forced to turn to his right during the forced-turn epoch had to choose a left-hand turn to win reward during the subsequent choice epoch. Forced-turn direction was varied randomly, with no more than three consecutive trials in one direction. Each rat was trained to asymptotic performance (~85% correct) over 12–14 days before surgery, then implanted with arrays of adjustable tetrode recording electrodes targeted to the mPFC (+3.2 mm, +0.6 mm from bregma), ipsilateral dorsal CA1 (+3.6 mm, +2.2 mm), and ventral CA1 (+6.3 mm, +6.2 mm). Differential recordings of thresholded extracellular action potentials and continuous LFP were made against a local reference electrode in overlying white matter (for CA1 recordings) or a proximal cortical region without spiking activity (mPFC). Theta was recorded in or near stratum pyramidale of CA1 (only LFP from dorsal CA1 was used for all analyses presented here). Action potentials were assigned to individual neurons by off-line, manual clustering using Xclust software (M.A. Wilson). Subsequent analyses employed a combination of in-house software (M.A. Wilson) and custom Matlab code (MathWorks, Natick, MA).

Each spike was assigned a position on the maze, and theta phase between 0 and 360°, as previously described (Siapas et al., 2005). Rayleigh's test of uniformity was used to test phase distributions for deviations from the circular uniform distribution. Circular statistics were calculated according to Fisher (1993). Higher values circular concentration coefficient, κ, correspond to narrower distributions around a mean preferred phase. Spikes from isolated neurons, or from multiunit activity, were binned into linear positional segments of ~2 cm in length to linearize firing rate plots.

Multitaper spectral analysis (Thompson, 1982) was used to calculate coherence between CA1 and mPFC central arm LFP sections. Coherence changes over time were converted to changes over position by extracting the positional sample closest in time to the center of each time bin used for the coherence calculation. Analyses consider only average coherence over the 4–12 Hz theta-frequency range, since these are the only frequencies at which we observed significant and consistent coherence under these conditions.

Phase precession of place cells in dentate gyrus, CA3, and CA1 on linear tracks is normally analyzed over the length of a cell's place field. As such, the field size imposes natural bounds on the times and positions over which precession can occur. However, the majority of mPFC units recorded during this task fired over relatively larger areas of the environment and did not exhibit unambiguous "place fields" (see Fig. 1C for example). We therefore restricted analyses of mPFC phase precession to runs across the central arm of the maze in the choice-turn direction. Running behavior and the theta rhythm itself were at their most uniform over this section of the maze. More importantly, we have previously shown hippocampal-prefrontal theta-frequency interactions to be at their peak during this choice-turn epoch of the task. We presumed that if mPFC phase precession is related to CA1 phase precession, then it was most likely to occur at these times of peak CA1-mPFC coordination.

Linear regression was used to quantify the position versus phase correlations that arise as a consequence of phase precession. For CA1 place cells with fields on the central arm of the maze ($n = 15$ in the choice direction), regression was restricted to the maximal linear segment of the position versus phase plot, determined by trial and error for each neuron (see Fig. 1B for example). The length of this segment proved quite variable, but on average corresponded to 20 ± 8.5 cm. To search for linear segments in mPFC position versus phase plots, we therefore applied linear regression to a 20-cm window stepped along the length of the central arm, calculating slope and Pearson's correlation coefficient (r^2) for each segment.

RESULTS

Figure 1B shows a typical example of phase-locking and phase precession in a CA1 place cell. Phase-locking is evident from the

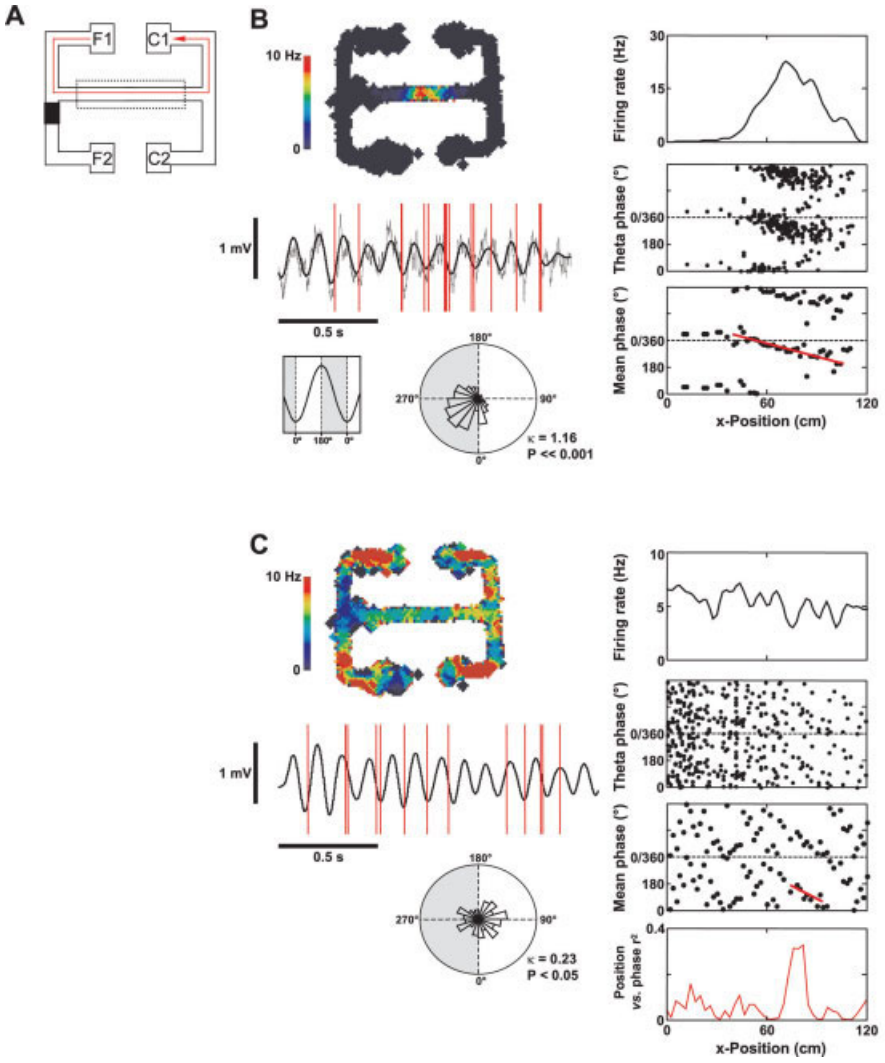

FIGURE 1. **A: Schematic of the end-to-end T-maze showing the moveable barrier at the forced-turn end. The red arrow marks an example of a correct trial run in the choice direction from reward point F1 to reward point C1. Data from F2 to C2 runs were also considered in the analyses. The dotted rectangle marks the central section of the central arm from which data were taken for firing rate, precession, and coherence analyses. B: Firing rate, phase-locking, and phase precession data for a single CA1 place cell. Spikes were binned into positional pixels and mean firing rate in each pixel color-coded to generate the firing-rate map. The raw LFP trace corresponds to one crossing of the central arm, with 4–12 Hz filtered LFP shown by the bold line and spike times of this neuron marked by the red vertical lines. The rose histogram shows the significantly nonuniform phase distribution of all spikes that fired during choice-direction runs across the central arm (κ, circular concentration coefficient, *P*-value for Rayleigh's test of uniformity). A reference theta-cycle is shown on the left. Graphs on the right show linearized central arm firing-rate with position (top), phase of each spike by position (middle), and circular mean phase by position (bottom). Phase plots are shown across two theta cycles for clarity; linear, diagonal sections correspond to regions of phase precession. The red line shows a linear regression fit (slope, -3.2° cm^{-1}; $r^2 = 0.46$). C: Equivalent firing-rate, phase-locking, and phase precession data for a single, simultaneously recorded mPFC neuron. Note the consistent phase precession toward the end of the central arm. This was quantified by linear regression of 20 cm segments of the data; corresponding Pearson's correlation coeffiecients (r^2) are shown in the bottom panel, with the fit for the best segment marked by the red line on the position versus phase plot (slope, -6.2° cm^{-1}; $r^2 = 0.30$).**

significantly nonuniform phase distribution of the neuron's spikes (circular concentration coefficient, $\kappa = 1.16$, deviation from uniform circular distribution $P \ll 0.001$ by Rayleigh's test). As the rat ran in the choice direction across the central arm of the maze (left to right in Fig. 1), firing rate increased in the neuron's place field and spikes occurred during progressively earlier phases of the theta cycle. Precession is therefore evident as a linear shift in preferred phase as the rat ran from left to right through the place field (slope, -3.1° cm^{-1}, $r^2 = 0.46$ in this example). Linear regression yielded a mean phase shift of $-7.6 \pm 3.6^\circ$ cm^{-1} ($r^2 = 0.54 \pm 0.11$, $n = 15$) for the hippocampal population on this section of the maze.

Figure 1C shows the equivalent analyses for a single, simultaneously recorded mPFC neuron. The firing rate map shows that this neuron fired over much larger areas of the maze than the CA1 place cell shown earlier, although it did demonstrate

some preference for firing on the reward arms of the maze. Firing on the central arm occurred at an approximately uniform rate of about 5 Hz during choice-direction runs. Like the CA1 place cell, phase-locking is demonstrated by the nonuniform phase distribution of spikes during choice-direction epochs ($\kappa = 0.23$, $P < 0.05$). Phase precession is perhaps less robust than in the CA1 example, but is again evident as a near-linear section of the position versus phase plot. The maximally linear segment of this plot (see Methods) had a slope of -6.2° cm^{-1} ($r^2 = 0.30$). Note that the section of the central arm with the clearest phase precession for this mPFC neuron coincides with the latter half of the arm, where the rat approached the decision point. The maximally linear segments of position versus phase plots for the mPFC population showed a mean phase shift of $-9.4 \pm 5.2^\circ$ cm^{-1} ($r^2 = 0.31 \pm 0.16$, $n = 39$). Thus, the correlations between position and phase were not as robust as for the hippocampal population, but were nevertheless within the hippocampal range.

mPFC precession did appear to differ from CA1 precession in two other respects. First, although the linear regression analysis identified unique segments of the most robust precession, precession did tend to occur over multiple segments spanning the central arm. Second, in contrast to the majority of reported CA1 data, mPFC precession spanned over 360° (see Tsodyks et al., 1996). Although we can only speculate as to mechanisms and implications, these CA1 versus mPFC differences may reflect the integration of a more diverse range of theta-modulated and phase-precessing inputs to mPFC (for example from CA1, subiculum, and entorhinal cortex) than are found in CA1.

Figure 2 shows mPFC population data from three different rats. Although mPFC firing rates did tend to fluctuate markedly (rates in Fig. 2A are Gaussian-smoothed for visualization, kernel width 8 cm), population firing rate ramped-up as the rats ran toward the choice point. Figure 3B shows that multiunit rates were significantly higher during the final third of the central arm relative to the first third of the arm (increasing by $9.0\% \pm 3.9\%$). The position versus phase plots in Figure 2B are for multiunit data: each point shows the mean preferred phase of the mPFC population at that position. It is remarkable, then, that the entire mPFC population showed evidence of coherent precession, with phase precessing toward 0° as the rats ran from left to right across the central arm. Although the precession tended to occur over the entire extent of the central arm (note the diagonal bands spanning the mean phase versus position plots, Fig. 2B), it was most linear on the second half of the arm (see increased correlation coefficients in this region in Fig. 2C).

The population mean preferred phase became more restricted—and the precession more apparent—as the rats reached the decision point at the end of the central arm. This restricted population phase preference is shown by the increasing population circular concentration coefficients at these positions (Fig. 2D). The mean population circular concentration coefficient increased significantly from 0.11 ± 0.07 on the first third of the central arm to 0.22 ± 0.07 on the last third (Fig. 3B).

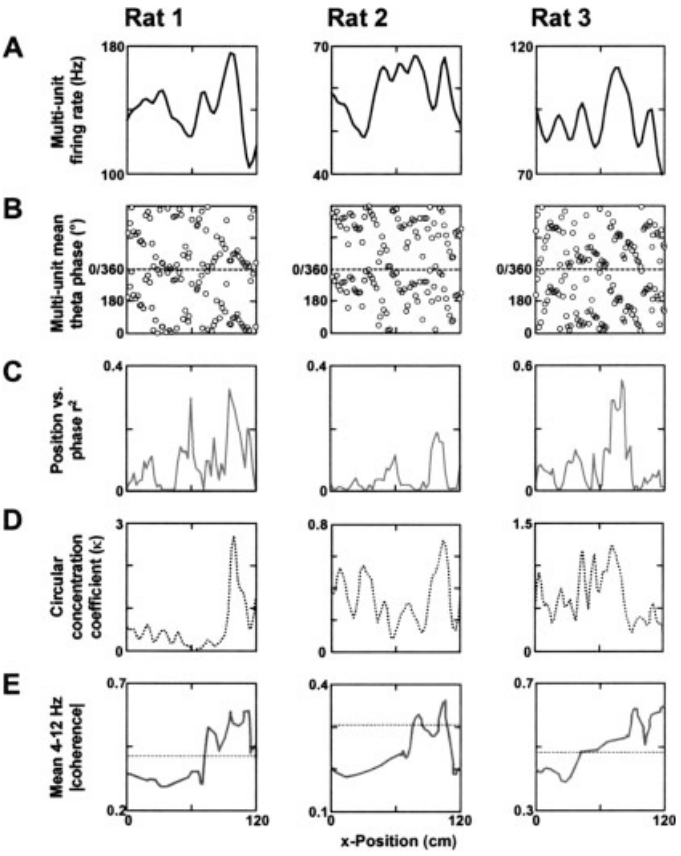

FIGURE 2. Prefrontal population firing rates (A), firing phase relative to CA1 theta (B), correlation coefficients for 20 cm linear regression segments (C), population circular concentration coefficients (D), and CA1-mPFC 4–12 Hz coherence magnitude (E) during runs across the central arm in the choice direction for three rats. Each point on the phase plots gives the circular mean phase of all spikes that fired within each positional bin. Dotted lines in (D) mark estimates of 95% confidence interval. Note that population firing rates, phase precession (evident as linear, diagonal sections of the phase plots and shown by the increased r^2 values in C), concentration around mean phase and theta-frequency coherence all increased in parallel as rats approached the choice point at the end of the central arm.

Consequently, the circular distributions of population mean preferred phase on the final third of the central arm were significantly nonuniform for 4 out of 4 rats; distributions on the initial third of the arm were significantly nonuniform in only 1 of 4 rats (see example in Fig. 3A). This effectively means that the range of theta phases over which mPFC neurons fired became more constrained toward the end of the central arm.

Figure 2E shows the magnitude of mean 4–12 Hz coherence between CA1 and mPFC LFP during choice epochs. Mean 4–12 Hz coherence was significantly higher on the final third of the central arm than the initial third (Fig. 3B; 0.46 ± 0.08 vs. 0.32 ± 0.06, respectively, $P < 0.05$). Increased theta-frequency coherence therefore paralleled the mPFC population's enhanced phase-locking and phase precession relative to the

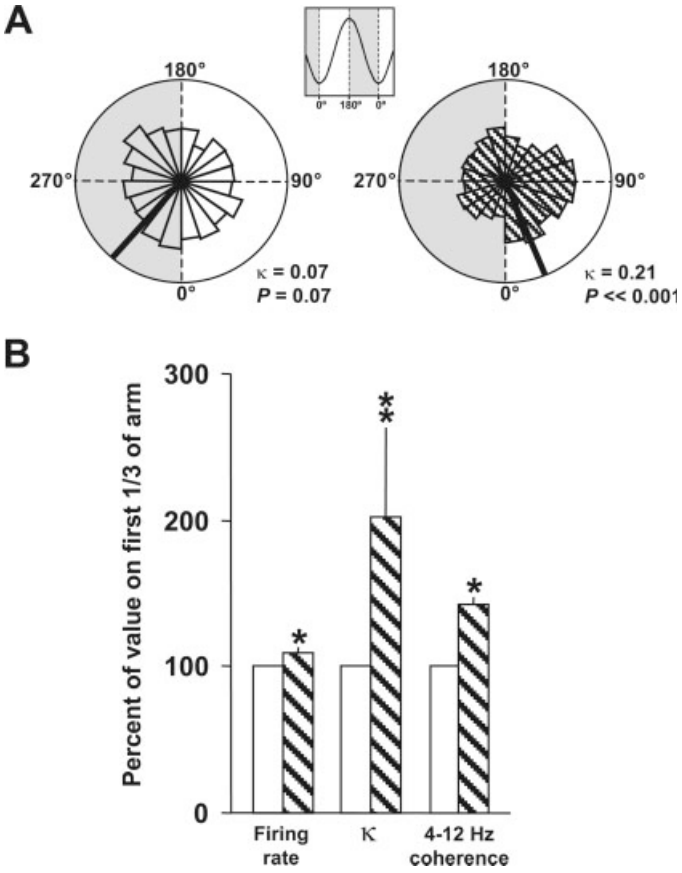

FIGURE 3. A: Phase distributions for mPFC population activity on the first third of the central arm (left, open segments) and the last third of the central arm (right, hatched segments) from Rat 1 (from Fig. 2). Note that the population distribution is only significantly nonuniform while the rat is on the last third of the arm, approaching the decision point. B: Mean data expressing mPFC population firing rates, circular concentration coefficients (κ) and theta-frequency coherence on the final third of the central arm (hatched bars) as a percentage of values on the first third of the arm (open bars). All three parameters significantly increased on the final third of the arm (*$P < 0.05$, **$P < 0.01$, two-tailed value from paired student's *t*-test).

CA1 theta rhythm as rats approached the decision point on the central arm of the maze.

DISCUSSION

It remains to be established whether mPFC phase precession is driven by CA1 phase precession, or whether it occurs independently. Monosynaptic projections from the hippocampus synapse onto both mPFC pyramidal cells and interneurons. For example, single-pulse stimulation of ventral CA1/subiculum evoked a monosynaptic excitatory response with a latency of ~15 ms the majority of mPFC pyramidal cells and interneurons tested by Degenetais et al. (2003) and Tierney et al. (2004). This pathway therefore provides the anatomical basis for hippocampal activity to drive mPFC activity with a temporal resolution sufficient to maintain phase precession. Siapas et al. (2005) suggested that hippocampal activity leads mPFC activity, since mPFC neurons lock more accurately to the preceding cycle of theta rhythm recorded in CA1 than to the coincident theta cycle. Together with our data showing that the clearest mPFC phase precession coincided with enhanced CA1-mPFC LFP coherence—and occurred at times when the behavior presumably demanded transfer of spatial information from CA1 to mPFC—this suggests that the precession is indeed a consequence of hippocampal input to the mPFC.

In the hippocampus, Harris et al. (2002) reported that the phase of each spike correlated well with the "instantaneous firing rate" of the cell at that time. Similarly, Mehta et al. (2002) suggested that ramping-up of excitatory input as animals move toward the peak of a cell's place field contributes to phase precession. Meanwhile, Huxter et al. (2003) claimed that correlations between phase and position were better than those between than phase and firing rate, and that the latter could therefore not entirely account for the former. We found no consistent evidence for a correlation between instantaneous firing rate and phase of mPFC neurons (data not shown). The mPFC integrates inputs from a broad range of sources; this anatomical and functional diversity may obscure the excitatory input/firing-rate/phase relationship more overtly evident in CA1. However, the multiunit firing rate of the mPFC population did tend to ramp-up as rats approached the choice end of the central arm, and may therefore contribute to the concomitant phase precession.

What are the functional implications of mPFC phase precession? Skaggs et al. (1996) suggested that phase precession in the hippocampus results in the reiteration of sequences of place cell activity that arise as rats pass through a series of overlapping place fields. Thus, as a rat passes through place fields of cells A→B→C→D, portions of the firing sequence ABCD are reiterated at a compressed timescale within concurrent theta cycles. The authors supposed that compression of firing sequences into sub-100-ms time windows would result in plasticity at synapses between the pre- and postsynaptic neurons involved, and that algorithm-like repetition of these sequences would reinforce such plasticity.

This hippocampal model was founded on the clear patterns of sequential place cell activity generated by locomotion through adjacent and overlapping place fields. Similar consequences of phase precession within the mPFC cannot be ruled out—although the firing of mPFC neurons is not overtly organized into discrete, sequential receptive fields, subsets of mPFC neurons certainly fire in an order imposed by behavior. However, simultaneous phase precession in CA1 and mPFC may also play a role in conserving sequential firing patterns across the two structures. By analogy with the hippocampal model, imagine that a rat moving across the central arm of the maze results in mPFC neuron A′ firing after place cell A on a behavioral timescale of 1–2 s. In order for the sequence A→A′ to be maintained in compressed form within each theta cycle during the two neurons' coactivity, the firing of mPFC neuron A′ must phase precess in parallel with the firing of place cell A. Indeed, although rates of precession were quite variable,

overall precession in degrees cm^{-1} occurred at a similar rate in both CA1 and mPFC. Thus mPFC phase precession may simply allow the temporal correlations between CA1 and mPFC spiking to be maintained. This is consistent with our work showing that ±100 ms cross-correlations between CA1-mPFC unit pairs are enhanced during choice-direction runs in this task (Jones and Wilson, 2005).

A striking feature of precession during this working memory task was that entire mPFC populations tended to precess coherently as rats crossed the central arm. As rats entered the initial section of the central arm, firing was dispersed over a large range of phases. In contrast, mPFC neurons fired within a more restricted phase window (in the early part of the theta cycle) as rats approached the decision point on the maze. It is not clear how or whether this convergence of mPFC firing onto earlier phases of the theta cycle relates to the precession. However, under these conditions a consequence of phase precession may be that population firing converges upon a more restricted phase during specific behavioral epochs (in this case converging upon earlier phases of the CA1 theta cycle toward the end of the central arm). It is not clear how this could arise from mPFC spike-timing passively "keeping up" with CA1 spike-timing in order to maintain correlations. These data therefore imply some active maintenance of mPFC preferred phase as a function of position or behavioral context. Regulation of mPFC network inhibition is one candidate mechanism that could control the firing phase of mPFC populations in parallel, rather than individually monitoring and controlling each neuron independently.

The relevance of the mPFC population activity converging around early phases of the CA1 theta rhythm toward the decision point is also unclear. One possibility is that the firing of place cells also converges around a similar phase at this point in space and time, thus establishing a time window (less than 1 theta cycle in duration) during which prefrontal and hippocampal neurons are more likely to be coactive. Unfortunately, few of the place cells recorded in this study were active at the end central arm, and we were unable to establish whether the CA1 population firing also precessed coherently and converged upon a population mean preferred phase.

We focused our search for mPFC phase precession on behavioral epochs that required rats to use spatial working memory to guide their imminent choice of turn direction. Under these conditions, we show that mPFC theta phase precession was evident both at the level of individual neurons and in mPFC multi-unit activity. To the best of our knowledge, this is the first report of theta phase precession outside the hippocampal formation. The mPFC precession was most consistent as rats approached the choice point at the end of the arm. These stretches of clear phase precession were accompanied by enhanced phase-locking—in the sense that the mPFC population tended to fire within a more concentrated window of theta phases—and enhanced theta-frequency coherence between CA1 and mPFC LFP. The causes and functions of phase precession remain unresolved. Nevertheless, its existence in structures anatomically and functionally connected to the hippocampus provides further evidence for a global role of theta rhythms in coordinating neuronal activity, and suggests that phase precession is a key mechanism or reflection of this coordination.

REFERENCES

Berke JD, Okatan M, Skurski J, Eichenbaum HB. 2004. Oscillatory entrainment of striatal neurons in freely moving rats. Neuron 43:883–896.

Bose A, Recce M. 2001. Phase precession and phase-locking of hippocampal pyramidal cells. Hippocampus 11:204–215.

Buzsaki G. 2002. Theta oscillations in the hippocampus. Neuron 33:325–340.

Buzsaki G, Eidelberg E. 1983. Phase relations of hippocampal projection cells and interneurons to theta activity in the anesthetized rat. Brain Res 266:334–339.

Colom LV, Christie BR, Bland BH. 1988. Cingulate cell discharge patterns related to hippocampal EEG, their modulation by muscarinic and nicotinic agents. Brain Res 460:329–338.

Degenetais E, Thierry AM, Glowinski J, Gioanni Y. 2003. Synaptic influence of hippocampus on pyramidal cells of the rat prefrontal cortex: an in vivo intracellular recording study. Cereb Cortex 13:782–792.

Fisher NI. 1993. Statistical analysis of circular data. Cambridge: Cambridge University Press.

Frank LM, Brown EN, Wilson MA. 2001. A comparison of the firing properties of putative excitatory and inhibitory neurons from CA1 and the entorhinal cortex. J Neurophysiol 86:2029–2040.

Harris KD, Henze DA, Hirase H, Leinekugel X, Dragoi G, Czurko A, Buzsaki G. 2002. Spike train dynamics predicts theta-related phase precession in hippocampal pyramidal cells. Nature 417:738–741.

Huxter J, Burgess N, O'Keefe J. 2003. Independent rate and temporal coding in hippocampal pyramidal cells. Nature 425:828–832.

Jensen O, Lisman JE. 1996. Hippocampal CA3 region predicts memory sequences: accounting for the phase precession of place cells. Learn Mem 3:279–287.

Jones MW, Wilson MA. 2005. Theta-frequency interactions between the hippocampus and medial prefrontal cortex during a spatial working memory task. Society for Neuroscience Abstracts.

Kahana MJ, Sekuler R, Caplan JB, Kirschen M, Madsen JR. 1999. Human theta oscillations exhibit task dependence during virtual maze navigation. Nature 399:781–784.

Lee H, Simpson GV, Logothetis NK, Rainer G. 2005. Phase locking of single neuron activity to theta oscillations during working memory in monkey extrastriate visual cortex. Neuron 45:147–156.

Lengyel M, Szatmary Z, Erdi P. 2003. Dynamically detuned oscillations account for the coupled rate and temporal code of place cell firing. Hippocampus 13:700–714.

Mehta MR, Lee AK, Wilson MA. 2002. Role of experience and oscillations in transforming a rate code into a temporal code. Nature 417:741–746.

O'Keefe J, Dostrovsky J. 1971. The hippocampus as a spatial map. Preliminary evidence from unit activity in the freely-moving rat. Brain Res 34:171–175.

O'Keefe J, Recce ML. 1993. Phase relationship between hippocampal place units and the EEG theta rhythm. Hippocampus 3:317–330.

Pare D, Gaudreau H. 1996. Projection cells and interneurons of the lateral and basolateral amygdala: distinct firing patterns and differential relation to theta and delta rhythms in conscious cats. J Neurosci 16:3334–3350.

Raghavachari S, Kahana MJ, Rizzuto DS, Caplan JB, Kirschen MP, Bourgeois B, Madsen JR, Lisman JE. 2001. Gating of human theta oscillations by a working memory task. J Neurosci 21: 3175–3183.

Siapas AG, Lubenov EV, Wilson MA. 2005. Prefrontal phase locking to hippocampal theta oscillations. Neuron 46:141–151.

Skaggs WE, McNaughton BL, Wilson MA, Barnes CA. 1996. Theta phase precession in hippocampal neuronal populations and the compression of temporal sequences. Hippocampus 6:149–172.

Thompson DJ. 1982. Spectrum estimation and harmonic analysis. Proc IEEE 70:1055–1996.

Tierney PL, Degenetais E, Thierry AM, Glowinski J, Gioanni Y. 2004. Influence of the hippocampus on interneurons of the rat prefrontal cortex. Eur J Neurosci 20:514–524.

Tsodyks MV, Skaggs WE, Sejnowski TJ, McNaughton BL. 1996. Population dynamics and theta rhythm phase precession of hippocampal place cell firing: a spiking neuron model. Hippocampus 6:271–280.

Vanderwolf CH. 1969. Hippocampal electrical activity and voluntary movement in the rat. Electroencephalogr Clin Neurophysiol 26:407–418.

Wallenstein GV, Hasselmo ME. 1997. GABAergic modulation of hippocampal population activity: sequence learning, place field development, and the phase precession effect. J Neurophysiol 78:393–408.

Wilson MA, McNaughton BL. 1993. Dynamics of the hippocampal ensemble code for space. Science 261:1055–1058.